

INFLUENCE OF s-d INTERFACIAL SCATTERING ON THE MAGNETORESISTANCE OF MAGNETIC TUNNEL JUNCTIONS

D. Bagrets^{1,2}, A. Bagrets², A. Vedyayev^{1,2}, and B. Dieny¹

¹CEA / Grenoble, Département de Recherche Fondamentale sur la Matière Condensée, SP2M / NM, 38054 Grenoble, France

²Département of Physics, M. V. Lomonosov Moscow State University, 119899 Moscow, Russia

The tunnel magnetoresistance (TMR) of spin-valve junctions of the form F/O/F where F's are transition metal ferromagnetic layers and O is an oxide spacer is theoretically investigated in the framework of s-d model. The generalized Kubo formalism and Green functions method together with the coherent potential approximation were used in order to investigate the influence of impurity and magnon interfacial scattering on the TMR magnitude. Based on the previous band-structure calculation, we assume that the exchange split quasi free electrons with the density of states greater for majority spin sub-band gives the main contribution to the TMR effect. We show that, due to the interfacial inter-band scattering, TMR can be substantially reduced even down to zero value. This is related to the fact that the delocalized quasi free electrons can scatter into strongly localized d sub-band, the density of states at Fermi level of which is larger for the minority spins compared to the majority spins. It is also shown that the presence of inelastic magnon scattering leads to a further decrease in the TMR magnitude at finite temperature.

PACS number(s): 75.70.-i, 73.40.Gk, 73.40.Rw, 85.30.Mn

I. INTRODUCTION

M. Julliere in 1975¹ observed, that the tunneling conductance of the three-layer system Fe/G e/C o depends on the angle between the magnetizations in the Fe and C o layers. The measured the amplitude of the tunnel magnetoresistance (TMR) was 14% at 4.2 K. Only 20 years later, the large TMR at room temperature was found in magnetic junctions comprising Al_2O_3 barrier^{2,4}. During the last ten years, a lot of theoretical papers were published on this topic (see reviews [5,6]). Experimentally it was observed that the TMR depends critically on the material of the insulating barrier and on the conditions of its preparation, in particular on the roughness of the interface between the metal and the insulating layer⁸. On the other hand, the first theory suggested by M. Julliere predicts no dependence at all of the value of TMR on the parameters of the barrier. In the subsequent theoretical papers^{9,10} it was shown that TMR amplitude depends on the height of the barrier and the effective mass of the tunneling electron inside the barrier. Later the TMR amplitude was calculated using the real band structure of the ferromagnetic layer in contact with insulating layer^{11,13}. One of the most important conclusions of all these papers is the observation that with Al_2O_3 barriers, mostly free-like sp-electrons give the essential contribution to the tunnel current and to the TMR, since they are exchange splitted. Strongly exchange splitted d-electrons are responsible for the ferromagnetism of the electrode layers but they give rather small contribution into the tunnel current. The authors of papers in Refs. [11-13] argue that the hopping integral across the F/O interface for d-electrons is much smaller than for sp ones. However, in

the case of $\text{Co/SrTiO}_3/\text{La}_{0.7}\text{Sr}_{0.3}\text{MnO}_3$ tunnel junction, as it was reported in Ref. [14], the situation is different and experiment shows that the d-electrons contribution into the tunnel current becomes dominant.

In Refs. [10,15] the influence of defects inside the barrier on the TMR was investigated. It was shown that usually they affect the polarization of the tunneling current so that TMR decreases. The effect of electron scattering at interfacial defects (so called impurity assisted tunneling) was theoretically investigated in [16,17]. In [16], the influence of spin- $\uparrow\downarrow$ scattering at the interface on the temperature and bias-voltage dependencies of TMR was investigated. It was shown that mixing of spin up and down tunnel channels leads to a decrease of the TMR. In Ref. [17] the processes with and without spin- $\uparrow\downarrow$ of the electron at the interfaces were examined in detail. It was shown that spin-conserving scattering may or may not lead to a decrease of TMR depending on the value of the amplitude of the scattering potential. The calculation in Ref. [17] was carried out for simple two-band (spin up and down) free-electron model. Simultaneously in the same paper¹⁷ it was noticed that if the s-d scattering at the interface is taken into account, it may lead to a substantial decrease of the TMR amplitude. However, no analytical treatment of such model exists so far. In this paper, we present the analytical investigation of the TMR in magnetic tunnel junctions taking into account the interfacial spin conserving s-d scattering as well as the spin- $\uparrow\downarrow$ processes. It is shown that if d-densities of states for spin up and down electrons are substantially different, which is always the case for 3d ferromagnetic metals, this scattering leads to a substantial decrease of TMR amplitude even at low temperatures.

II. THEORETICAL MODEL

A. Hamiltonian of the system

The system under investigation is a three-layer sandwich of the form $F_1/O/F_2$, where F_1 and F_2 represent two semi-infinite ferromagnetic layers and O is a dielectric oxide spacer (Al_2O_3). It is assumed, that electrons in ferromagnetic layers are described as free-electron gas, but two types of charge carriers exist. Namely, according to Steams model of electron tunneling¹⁸, we consider the almost free-like electrons from s and d hybridized bands as s -like electrons with effective mass $m_s \approx m_e$. In her original paper¹⁸, Steams designated these electrons as itinerant d_i electrons. We denote other more localized electrons as d -like electrons, with effective mass $m_d \approx m_s$. Both s and d -sub-bands are exchange splitted, with exchange energies $W_s^{exch} = W_d^{exch} = W$, where W 's are the widths of the bands. It is supposed that interfaces F/O and O/F are rough and possibly contaminated by some amount of impurities. These structural defects are characterized by random potentials, which may be divided in two terms: spin-conserving and spin- $\uparrow\downarrow$ ones. The plane parallel to the interface is the xy -plane and the axis perpendicular to the interface is the z -axis. Let $z_1 = a$ and $z_2 = b$ be the positions of interfaces (see Fig. 1). The Hamiltonian of the system is written as:

$$\hat{H} = \hat{H}_0 + \hat{H}_{\text{spin-cons}} + \hat{H}_{\text{spin-}\uparrow\downarrow}; \quad (1)$$

with

$$\hat{H}_0 = \int_{-\infty}^{\infty} dz \int_{-\infty}^{\infty} dr \left[\psi_s^\dagger(r) \left(-\frac{\hbar^2}{2m_s(z)} \nabla^2 + U^s(z) \right) \psi_s(r) + \psi_d^\dagger(r) \left(-\frac{\hbar^2}{2m_d(z)} \nabla^2 + U^d(z) \right) \psi_d(r) \right];$$

$$\hat{H}_{\text{spin-cons}} = \sum_{n=1,2} \sum_{\sigma=\uparrow,\downarrow} \int_{-\infty}^{\infty} dz \int_{-\infty}^{\infty} dr \left[\psi_{s\sigma}^\dagger(r) \hat{S}_z \psi_{s\sigma}(r) + \psi_{d\sigma}^\dagger(r) \hat{S}_z \psi_{d\sigma}(r) \right];$$

$$\hat{H}_{\text{spin-}\uparrow\downarrow} = \sum_{n=1,2} \sum_{\sigma=\uparrow,\downarrow} \int_{-\infty}^{\infty} dz \int_{-\infty}^{\infty} dr \left[\psi_{s\sigma}^\dagger(r) \hat{S}_+ \psi_{d\sigma}(r) + \psi_{d\sigma}^\dagger(r) \hat{S}_- \psi_{s\sigma}(r) \right];$$

Here $\sigma = \uparrow, \downarrow$ is electron spin; $\psi_s^\dagger(r)$, $\psi_d^\dagger(r)$ and $\psi_s(r)$, $\psi_d(r)$ are field operators of creation and annihilation of s and d -type electrons with spin σ at point r . We suppose that both s and d -like electrons can penetrate into the insulator layer, and their effective masses $m_s(z)$ and $m_d(z)$ may be different in the ferromagnetic layer (m_s^0 and m_d^0) and in the oxide layer (m_s^0 and m_d^0). $U^s(z)$, $U^d(z)$ are spin-dependent model step-like potentials of s and d -bands shown in Fig. 1:

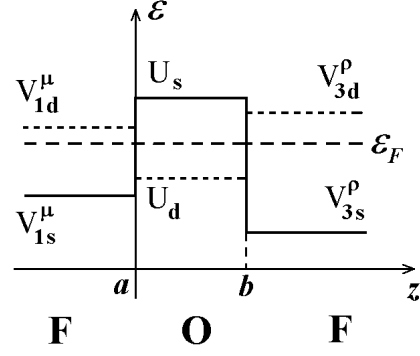


FIG. 1. The model potentials describing the propagation of an electron in the three-layer structure $F/O/F$. The solid line corresponds to the potential profile of s -like electrons and the dashed line for d -like electrons. $V_{1(3)}^{(\cdot)}$ denote the spin-dependent band bottoms, U is the height of the potential barrier and ϵ_F is Fermi level.

$$U^s(z) = \begin{cases} 0 & z < a \\ U_s & a < z < b \\ 0 & z > b; \end{cases}$$

$$U^d(z) = \begin{cases} 0 & z < a \\ U_d & a < z < b \\ 0 & z > b; \end{cases}$$

where V_{is} , V_{id} ($i = 1, 3$) are spin-dependent band bottoms in ferromagnetic layers, U_s and U_d are the heights of the potential barriers. The concrete values of the effective electron masses and parameters describing them model potentials will be pointed out in section III. Here we only remind that according to typical band structure of 3d transition metals like Fe, Co and Ni, the narrow minority and majority bands corresponding to more localized electron states are practically filled¹⁹ and thus in the present model the charge carriers with large effective mass should be regarded as holes, so the Fermi energy level is situated with respect to profiles of the potentials $U^s(z)$ and $U^d(z)$ as it is indicated in Fig. 1.

$\hat{H}_{\text{spin-cons}}$ is the spin-conserving part of the Hamiltonian, $n = 1, 2$ being the interface numbers. We shall describe the interface structure similar to the well-known s - d model for ferromagnetic binary alloys of a type A_xB_{1-x} developed in Ref. [20], i.e. the roughness is modeled by the disordered "alloy" with the random parameter ϵ_n of s - d hybridization at site n , assuming two different values ϵ_A and ϵ_B with the probabilities x and $(1-x)$, respectively, where A corresponds to metal atoms and B corresponds to "oxide" ones.

$\hat{H}_{\text{spin-}\uparrow\downarrow}$ is a part of Hamiltonian related to the spin- $\uparrow\downarrow$ processes only for s -like electrons, since they are itinerant and give the most essential contribution to the tunneling current. Operators $\hat{S}_+^{(\sigma)}$, $\hat{S}_-^{(\sigma)}$ are defined as

$$\hat{S}_+ (n) = \frac{1}{2SN} \sum_q e^{iq_n} b_q;$$

$$\hat{S}_- (n) = \frac{1}{2SN} \sum_q e^{iq_n} b_q^\dagger;$$

Here b_q^\dagger, b_q denotes the creation and annihilation operators corresponding to surface magnons, N is number of lattice sites at the interface, S is spin number. J_n is a random exchange integral which also assumes the values J_A and J_B with probabilities x and $(1-x)$. We suppose that the disorder is uncorrelated between different

interfaces, i.e. $\langle J_n^{(1)} J_m^{(2)} \rangle = 0$ and $\langle J_n^{(1)} J_m^{(2)} \rangle = 0$, and furthermore that J_n and J_m are also uncorrelated between different sites of the same interface, i.e. $\langle J_n J_m \rangle = 0$ and $\langle J_n J_m \rangle = 0$, if $m \neq n$.

B. The calculation of the conductance of the system

The non-local conductivity of the system is calculated in accordance with Kubo formula of the linear response²¹:

$$\langle r; r^0 \rangle = \frac{1}{4} \frac{e}{h} \frac{1}{2m} \sum_{ss'} \text{Sp} \left[G^R(r; r^0) \hat{r}_r \hat{r}_{r^0} G^A(r^0; r) + G^A(r; r^0) \hat{r}_r \hat{r}_{r^0} G^R(r^0; r) \right]; \quad (2)$$

where $\hat{r}_r = (\hat{r}_r, \hat{r}_r)$ is asymmetric gradient operator, $G^R(r; r^0)$ and $G^A(r; r^0)$ are the retarded and advanced (2-2) matrix Green functions (with components ss, sd, ds and dd), $\hat{r}_r = \hat{r}_r / \hbar$ are the projections of spin of the electrons, \hat{r}_r denote the averaging over the configurations and magnon degrees of freedom, the trace (Sp) is going over s and d indices of the bands.

To calculate the conductance (2) of the system we have to find the Green function of the Hamiltonian (1), which can be found by solving the following system of differential equations in the mixed $(z; z^0)$ representation²²:

$$\sum_{ss'} \hat{H}^i(z) G^i(z; z^0) = \delta(z - z^0) \quad (3)$$

$i = s; d$

$$\hat{H}^i(z) = \frac{\hbar^2}{2m} \frac{\partial^2}{\partial z^2} + \frac{U}{2m} + U(z) + (a)(z-a) + (b)(z-b); \quad (4)$$

where Greek indices i, j and k assume values s and d , i denotes the electron's spin, \hat{r}_r is a projection of the electron's momentum to the xy -plane. $\hat{H}^i(z)$ is (2-2) matrix linear differential operator where (a) and (b) ($i = s; d$; $\hat{r}_r = \hat{r}_r / \hbar$) denote the coherent potentials for up and down electrons which take into account the scattering of electron by the random spin-conserving and spin- $\uparrow\downarrow$ potentials on the interfaces. They are calculated using the well-known coherent potential approximation (CPA)²³, the details of these calculations are presented in the subsequent section IIC. Operator $\hat{H}^i(z)$ represents the effective single-particle Hamiltonian of the system which is, however, non-Hermitian since coherent potentials are imaginary numbers.

In order to solve Eq. (3) for Green functions, we shall follow the procedure described below. First of all, let's solve the Shrodinger equation with Hamiltonian $\hat{H}^i(z)$:

$$\sum_{ss'} \hat{H}^i(z) \psi^i(z) = 0; \quad (5)$$

$i = s; d$

This equation can be easily solved since the potentials $U(z)$ have step-like form. Let us put $U = U_F + i0$, where U_F is Fermi energy, and introduce the following notations: $k_{1s}^F = \frac{2m_s(U_F - V_{1s})}{\hbar^2}$, $k_{3s}^F = \frac{2m_s(U_F - V_{3s})}{\hbar^2}$, $k_{1d}^F = \frac{2m_d(U_F - V_{1d})}{\hbar^2}$, $k_{3d}^F = \frac{2m_d(U_F - V_{3d})}{\hbar^2}$ are Fermi momenta in F_1 and F_3 ferromagnetic layers, $q_s^F = \frac{2m_s^0(U_s - U_F)}{\hbar^2}$, $q_d^F = \frac{2m_d^0(U_d - U_F)}{\hbar^2}$ are Fermi momenta in the oxide. Let also $k_1 = k_{1s}^F$ and $k_3 = k_{3s}^F$ be the components of electron's momentum with spin along z -axis in F_1 and F_3 layers, respectively (\hat{r}_r is in-plane component of the momentum, i is a band index), and let $q_2 = \frac{q_s^F + q_d^F}{2}$ be the imaginary electron's momentum in the dielectric layer.

Hereafter, for convenience, we shall omit indices i and j in the notation of some functions. Equation (5) has four linear-independent solutions which we denote as

$$\psi_i(z) = \begin{cases} \psi_i^s(z) \\ \psi_i^d(z) \end{cases} \quad (i = 1; 2)$$

and

$$\psi'_i(z) = \begin{cases} \psi_i^s(z) \\ \psi_i^d(z) \end{cases} \quad (i = 1; 2);$$

We choose these independent solutions in such a way that two functions $\psi_1(z)$ and $\psi'_1(z)$ describe two waves corresponding to the s -like electrons, and functions $\psi_2(z)$ and $\psi'_2(z)$ correspond to d -like electrons. Namely, in F_1 layer ($z < a$) the solutions $\psi'_i(z)$ have the form

$$\psi'_1(z) = \exp[-ik_1^s z] \quad z < a; \quad (6)$$

$$\psi'_2(z) = \exp[-ik_1^d z] \quad z < a;$$

and in F_3 layer ($z > b$) the solutions $\psi_i(z)$ are

$$\psi_1(z) = \exp[ik_3^s z] \quad z > b; \quad (7)$$

$$\psi_2(z) = \exp[ik_3^d z] \quad z > b;$$

Since $\epsilon = \epsilon_F + i0$, we have $\text{Im } k_i = +0$ ($i = 1; 2$; $= s; d$). Thus these solutions satisfy the following boundary conditions:

$$\begin{aligned} \psi_i(z) & \rightarrow 0 \quad \text{if } z \rightarrow +1 \quad (i = 1; 2); \\ \psi'_i(z) & \rightarrow 0 \quad \text{if } z \rightarrow -1 \quad (i = 1; 2); \end{aligned}$$

Starting from expressions (6) and (7), the solutions $\psi'_i(z)$, $\psi_i(z)$ can be easily built in the two other layers. Let us introduce the matrices

$$D(z) = \begin{pmatrix} \psi_1^s(z) & \psi_2^s(z) \\ \psi_1^d(z) & \psi_2^d(z) \end{pmatrix};$$

$$D(z) = \begin{pmatrix} \psi_1^s(z) & \psi_2^s(z) \\ \psi_1^d(z) & \psi_2^d(z) \end{pmatrix};$$

and let \hat{D}_z be the matrix operator of the form

$$\hat{D}_z = \begin{pmatrix} 0 & 1 \\ \frac{1}{2m_s(z)} \frac{\partial}{\partial z} & 0 \\ 0 & \frac{1}{2m_d(z)} \frac{\partial}{\partial z} \end{pmatrix} \begin{pmatrix} B \\ C \\ A \end{pmatrix};$$

The Wronskian of the system (5) is

$$W = {}^T(z) \hat{D}_z(z); \quad (8)$$

The subscript T here designates the transposition operation. As it is known from the theory of differential equations, matrix W is constant, since it satisfies the relation $\frac{\partial W}{\partial z} = 0$. Then, taking into account that $\epsilon = \epsilon_F + i0$ and $\text{Im } k_i < 0$, the solution of Eq. (3) for retarded Green function in the matrix form can be written as

$$\begin{aligned} G^R(z; z^0) &= D(z) [{}^T(z)]^{-1} {}^T(z^0); \quad \text{if } z < z^0 \\ G^R(z; z^0) &= D(z) {}^T(z^0); \quad \text{if } z > z^0; \end{aligned} \quad (9)$$

To find the advanced Green function, we have to put $\epsilon = \epsilon_F - i0$ in Eq. (3) and assume that $\text{Im } k_i > 0$. Then we obtain

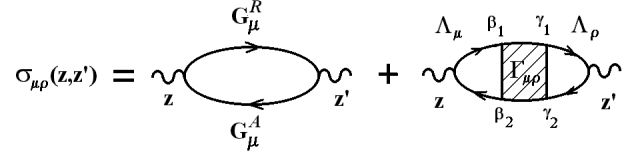


FIG. 2. The diagrammatic representation of the total two-point nonlocal conductivity $\sigma_{\mu\rho}(z; z^0)$ as a sum of "bubble" and "vertex" parts. Here the full lines correspond to Green functions $G^R(z; z^0)$, $G^A(z; z^0)$, and wavy lines denote an asymmetric gradient operator r_z of velocity at points z and z^0 . The shaded square designates the vertex part at the interface.

$$G^A(z; z^0) = G^R(z; z^0); \quad (10)$$

In the above expressions (9) and (10) the Green functions depend on the in-plane momentum and on the spin of the electron because solutions $\psi_i(z)$ and $\psi'_i(z)$ also depend on σ and s .

To proceed further, one has to compute the two-point conductivity (2) of the system using the Green functions (9) and (10). For this goal, we introduce current matrices j and j' ($\sigma = s; d$) constructed on the solutions $\psi_i(z)$ and $\psi'_i(z)$, respectively:

$$\begin{aligned} j(z) &= \psi^s(z) \hat{D}_z(z); \\ j'(z) &= \psi^d(z) \hat{D}_z(z); \end{aligned} \quad (11)$$

The total conductance of the system $\sigma(z; z^0)$ may be presented in the usual form as a sum of "bubble" part and the contribution from the vertex correction (see Fig. 2)²⁴:

$$\sigma(z; z^0) = \sigma^0(z; z^0) + \sigma^a(z; z^0) + \sigma^b(z; z^0); \quad (12)$$

Substituting the obtained expressions (9), (10) for Green functions and using the definition (11) for the current matrices, we come to the following results. The analytical expression for the "bubble" conductance is given by

$$\sigma^0(z; z^0) = \frac{e^2}{2hS} \text{Sp} \left(\frac{1}{j'(z)} {}^T \frac{1}{j(z^0)} \right); \quad (13)$$

here S is the Wronskian (8), S denotes the junction area.

The contribution due to vertex correction from the left and right interfaces can be written as

$$\sigma^a(z; z^0) = \frac{e^2}{2hS^2} \text{Sp} \left(\frac{1}{j'(z)} {}^T \frac{1}{j(z^0)} \right) \sigma^0(a; z^0); \quad (14)$$

$$b(z; z^0) = \frac{e^2}{2 \hbar S^2} \sum_0^n \text{Sp} \left(\begin{matrix} 1 & 2 \\ 2 & 2 \end{matrix} (z; b) \begin{matrix} 1 & 1 \\ 2 & 2 \end{matrix} \begin{matrix} 1 & 2 \\ 0 & 2 \end{matrix} (b; z^0) \right)^0 ;$$

where also is performed the sum over repeating indices $i; i = s; d$. Here $\begin{matrix} 1 & 1 \\ 2 & 2 \end{matrix}$ and $\begin{matrix} 1 & 1 \\ 2 & 2 \end{matrix}$ are vertex parts on the interfaces a and b . $\begin{matrix} 1 & 2 \\ 2 & 2 \end{matrix}$ are matrices, their components are defined by

$$\begin{aligned} \begin{matrix} 1 & 2 \\ 2 & 2 \end{matrix} (z; a) &= \text{Sp} \left(\frac{1}{y} j'^T(z) \frac{1}{y} \begin{matrix} 1 & 2 \\ 2 & 2 \end{matrix} (a) \begin{matrix} 1 & 2 \\ 2 & 2 \end{matrix} \right); \quad (15) \\ \begin{matrix} 1 & 2 \\ 2 & 2 \end{matrix} (a; z^0) &= \text{Sp} \left(\frac{1}{y} j'^T(a) \begin{matrix} 1 & 2 \\ 2 & 2 \end{matrix} \frac{1}{y} j(z^0) \right); \end{aligned}$$

where $\begin{matrix} 1 & 2 \\ 2 & 2 \end{matrix} (a)$ and $j'^T(a) \begin{matrix} 1 & 2 \\ 2 & 2 \end{matrix}$ are density matrices with components:

$$\begin{aligned} \begin{matrix} 1 & 2 \\ ik & ik \end{matrix} &= \begin{matrix} 1 & 1 \\ i & i \end{matrix} (a) \begin{matrix} 2 & 2 \\ k & k \end{matrix} (a) \quad (i; k = s; d); \quad (16) \\ j'^T(a) \begin{matrix} 1 & 2 \\ ik & ik \end{matrix} &= j'^T(a) \begin{matrix} 1 & 1 \\ i & i \end{matrix} \begin{matrix} 2 & 2 \\ k & k \end{matrix} (a) \quad (i; k = s; d); \end{aligned}$$

The expressions similar to expressions (15) may be also written for matrices $\begin{matrix} 1 & 2 \\ 2 & 2 \end{matrix} (z; b)$ and $\begin{matrix} 1 & 2 \\ 2 & 2 \end{matrix} (b; z^0)$. The vertex parts $\begin{matrix} 1 & 1 \\ 2 & 2 \end{matrix}$ and $\begin{matrix} 1 & 1 \\ 2 & 2 \end{matrix}$ have been calculated in the present work in the "ladder" approximation²⁵. The details of derivation of the expression for $\begin{matrix} 1 & 2 \\ 2 & 2 \end{matrix}$ are presented in the subsection IID.

We point out here on important point, that the coherent potentials $\begin{matrix} 1 & 2 \\ 2 & 2 \end{matrix} (a)$, $\begin{matrix} 1 & 2 \\ 2 & 2 \end{matrix} (b)$ calculated in the framework of CPA and vertices $\begin{matrix} 1 & 1 \\ 2 & 2 \end{matrix}$, $\begin{matrix} 1 & 1 \\ 2 & 2 \end{matrix}$ calculated in the "ladder" approximation satisfy the so-called Ward's identity which in our case, for example, for the interface $z = a$ can be written as (for the details, see Appendix A):

$$\begin{aligned} G(a) &= \begin{matrix} 0 & 1 \\ \begin{matrix} B \\ B \\ C \end{matrix} & \begin{matrix} \frac{ik_1^s}{2m_s} & \frac{q_2^s}{2m_s^0} \end{matrix} \end{matrix} \begin{matrix} ss(a) \\ ds(a) \end{matrix} \begin{matrix} 1 & 1 \\ \begin{matrix} C \\ C \\ A \end{matrix} & \begin{matrix} sd(a) \\ dd(a) \end{matrix} \end{matrix}; \\ G(b) &= \begin{matrix} 0 & 1 \\ \begin{matrix} B \\ B \\ C \end{matrix} & \begin{matrix} \frac{ik_3^s}{2m_s} & \frac{q_2^s}{2m_s^0} \end{matrix} \end{matrix} \begin{matrix} ss(b) \\ ds(b) \end{matrix} \begin{matrix} 1 & 1 \\ \begin{matrix} C \\ C \\ A \end{matrix} & \begin{matrix} sd(b) \\ dd(b) \end{matrix} \end{matrix} : \quad (19) \end{aligned}$$

Here m and m^0 ($= s; d$) are the effective electron masses in ferromagnetic and oxide layers; k_i and q_i ($i = 1; 3$, $= s; d$) are functions on ϵ introduced above in the text after Eq. (5). Let us define the "transport" density of states as follows:

$$\begin{aligned} A(a) &= G^y(a) j^T G(a); \\ A(b) &= G^y(b) j^T G(b); \quad (20) \end{aligned}$$

where

$$\begin{aligned} \text{Im} \begin{matrix} 1 & 2 \\ 2 & 2 \end{matrix} (a) &= \sum_a \begin{matrix} 1 & 1 \\ 2 & 2 \end{matrix} \frac{1}{S} \sum_n \text{Im} G \begin{matrix} 1 & 2 \\ 2 & 2 \end{matrix} (a) \\ &= \sum_a \sum_n G \begin{matrix} 1 & 1 \\ 2 & 2 \end{matrix} (a) G \begin{matrix} 2 & 2 \\ 2 & 2 \end{matrix} (a) \text{Im} \begin{matrix} 1 & 2 \\ 2 & 2 \end{matrix} (a) : \quad (17) \end{aligned}$$

Here the sum over repeating indices i and i is also performed. The fulfillment of (17) provides the necessary condition of the nondivergency of the current through the system:

$$\frac{\partial}{\partial z^0} \begin{matrix} 1 & 2 \\ 2 & 2 \end{matrix} (z; z^0) + \frac{\partial}{\partial z^0} \sum_a \begin{matrix} 1 & 2 \\ 2 & 2 \end{matrix} (a; z; z^0) + \sum_b \begin{matrix} 1 & 2 \\ 2 & 2 \end{matrix} (b; z; z^0) = 0: \quad (18)$$

According to expression (18), the total conductance of the system is a constant value. In view of this, we shall derive exact expression for $\begin{matrix} 1 & 2 \\ 2 & 2 \end{matrix} (z; z^0)$ computing the conductance at points $z = a + 0$ and $z^0 = b + 0$, i.e. at the left and at the right sides from the interface. The Wronskian matrix and matrices of current $j^T(z)$ and $j(z^0)$ are expressed in terms of matrices $\begin{matrix} 1 & 2 \\ 2 & 2 \end{matrix} (z)$ and $\begin{matrix} 1 & 2 \\ 2 & 2 \end{matrix} (z^0)$ these matrices, as follows from Exp. (9), determine the Green function. Thus, the straightforward computation of the conductance according to formulae (13)-(15) leads to the result that $\begin{matrix} 1 & 2 \\ 2 & 2 \end{matrix} (a; b)$ is expressed in terms of retarded Green functions $G(a) = G^R(z = z^0 = a)$ and $G(b) = G^R(z = z^0 = b)$ at the points of interfaces constructed according to formula (9). The explicit form of these Green functions in $(\epsilon; z)$ representation is given by the expressions:

$$\mathbf{j}' = \begin{pmatrix} 0 & 1 \\ \frac{k_1^s}{m_s} & 0 \\ 0 & \frac{k_1^d}{m_d} \end{pmatrix} \mathbf{C} \mathbf{A}; \quad \mathbf{j} = \begin{pmatrix} 0 & 1 \\ \frac{k_3^s}{m_s} & 0 \\ 0 & \frac{k_3^d}{m_d} \end{pmatrix} \mathbf{C} \mathbf{A} :$$

Expression (13) for the "bubble" conductance then reads

$$G^0(a;b) = \frac{e^2}{2\hbar S} \text{Sp} \frac{\hat{q}}{m} \mathbf{A}^T(a) \frac{\hat{q}}{m} \mathbf{A}(b); \quad (21)$$

where

$$\frac{\hat{q}}{m} = \begin{pmatrix} 0 & 1 \\ \frac{q_2^s}{m_s} e^{iq_2^s(b-a)} & 0 \\ 0 & \frac{q_2^d}{m_d} e^{iq_2^d(b-a)} \end{pmatrix} \mathbf{C} \mathbf{A} :$$

For the contribution to the vertex correction from the left interface at point $z = a$ we obtain

$$G^a(a;b) = \frac{e^2}{2\hbar S^2} \text{Sp} \frac{\hat{q}}{m} \mathbf{A}^T(a) \frac{\hat{q}}{m} \mathbf{A}(b) \mathbf{G}^Y(a); \quad (22)$$

$$\mathbf{G}^a(a;a) = \mathbf{A}(a); \quad \mathbf{G}^a(a;b) = \mathbf{G}^Y(a) \frac{\hat{q}}{m} \mathbf{A}(b) \frac{\hat{q}}{m} \mathbf{G}^Y(a);$$

In the similar way, the contribution to the vertex correction from the right interface at point $z = b$ reads as

$$G^b(a;b) = \frac{e^2}{2\hbar S^2} \text{Sp} \frac{\hat{q}}{m} \mathbf{A}^T(a) \frac{\hat{q}}{m} \mathbf{A}(b) \mathbf{G}^X(b); \quad (23)$$

$$\mathbf{G}^b(a;b) = \mathbf{G}^X(b) \frac{\hat{q}}{m} \mathbf{A}(a) \frac{\hat{q}}{m} \mathbf{G}^X(b); \quad \mathbf{G}^b(b;b) = \mathbf{A}(b);$$

Expressions (21)-(23) determine the total conductance of the system and are the final result of this section.

C. The CPA equations

In this section we derive the self-consistent equations of the coherent potential approximation²³ (CPA) for the case of the 2-D dimensional interfaces which have been used to obtain the self-energies $\Sigma^a(a)$ and $\Sigma^b(b)$ in the effective one-electron Hamiltonian (4) and in the calculation of the interfacial Green functions of the system (19). Our way of the representation of the CPA equations in the elegant analytical form which is convenient for the numerical iterative procedure will be based on the augmented space formalism by Mookerjee²⁶. After that we shall formulate the equation of the "ladder" approximation by Velicky²⁵ for our particular case that determine the vertex part \mathbf{G}^a and \mathbf{G}^b which are necessary to calculate the dissipative part of the conductance of the system.

Originally, the CPA is a self-consistent single site approximation, which is used to describe the propagation of an electron through the random media with a quenched disorder and due to that is related only with elastic random scattering. In our particular study, we intend to include into the self-energy operator the effects of both (i) the random s-d hybridization caused by interfacial roughness and (ii) random spin- \uparrow magnon scattering of itinerant s-like electrons [see Hamiltonian (1)]. While the first part of the random potential $\hat{H}_{\text{spin-cons}}$ is

related with elastic scattering, the second one $\hat{H}_{\text{spin-}\uparrow}$ may be in general the source of inelastic scattering due to the absorption or emission of some amount of energy from magnetic excitation in the system. But for the purposes of the present work, it is not of the great importance to take into account this possible inelastic nature of electron-magnon scattering and it will be treated in the static approximation. The procedure of averaging over impurities configurations and magnon degrees of freedom will be defined more exactly later in the text. This approach enables us to apply the CPA approximation for the determination of the self-energy in question.

We define the kets $|j; i; j_n\rangle$ corresponding to the Wannier state of an electron at the $n = 1, 2$ interface at the given site j_n in the (x, y) plane, where j refers to orbital states s or d and i is spin. The symbol \otimes denotes the direct product which shows that this given vector from the basis set at the interface can be decomposed into spatial part $|j_n\rangle$ and the vector $|j; i\rangle$ of the orbital and spin degrees of freedom. Then, in the view of preceding discussion, we reduce the problem of finding the one-particle Green function $G(r; r')$ of the many-body Hamiltonian (1) to the related one-electron problem of the propagation of electron in the random interfacial potential

$$V = \sum_{n; j=1,2} |j_n\rangle \hat{v}_n^{(el)} + \hat{v}_n^{(sf)} |h_n\rangle = \sum_{n; j=1,2} |j_n\rangle \hat{v}_n |h_n\rangle$$

where $\hat{v}_n = \hat{v}_n^{(el)} + \hat{v}_n^{(sf)}$ and the sum is going over the interface number n and the site n .

$$\hat{v}_n^{(el)} = \sum_{j; i; d} f_{j; i; d} \hat{h}_{j; i; d} + \sum_{j; i; s} h_{j; i; s} \hat{g}_{j; i; s} \quad (24)$$

is the random potential of s-d hybridization at site n and

$$\hat{v}_n^{(sf)} = J_n \sum_{j; i; s} \hat{S}_{-}(n) \hat{h}_{j; i; s} + \sum_{j; i; s} \hat{S}_{+}(n) \hat{h}_{j; i; s} \quad (25)$$

is the exchange-like interaction with the random Bose field of magnon subsystem. The random quantities \hat{v}_n and J_n used here are the same as they were introduced in Section II A.

One can now formulate the CPA procedure by the ordinary way and the only difference with respect to the usual situation of bulk scattering is that initial Green functions have to be calculated for the three-layer system. We assume, that the averaged propagator of the system $G(r; r^0)$, differs from the initial Green function of the system, corresponding to the Hamiltonian \hat{H}_0 [see Exp. (1)], by the self-energy correction in Eq. (3, 4). This means that the system behaves as if coherent potentials

had been assigned to each site of the interface a and b. From the other hand, the random potential \hat{v}_n at the n site looks like a source of the effective random potential $\hat{u}_n = \hat{v}_n$. It will produce scattering over the effective media with an apparent single-site t-matrix

$$\hat{t}_n = \frac{1}{1 - f \hat{v}_n} f \hat{v}_n \hat{g}(z) \quad (26)$$

where $z = a$ or b ,

$$\hat{g}(z) = \sum_{j; i} \hat{h}_{j; i}(z) \hat{g}_{j; i}(z) \quad (27)$$

Here

$$G(z) = \int_0^{Z_{max}} G(z; \frac{d}{2}) \quad (28)$$

is the averaged Green function at the interface which is expressed via \hat{g} in accordance with (19). Z_{max} is a cut-off in plane momentum which originates from the finite size of the Brillouin zone and is necessary to avoid divergency on the upper limit of the integral. For that, we have substituted the Brillouin zone's projection onto $(k_x; k_y)$ plane by the circle of the same square with radius $Z_{max} = 2 \frac{d}{2} = 2a_0$ corresponding to bcc lattice of Fe electrodes. The single-site t-matrix (26) is obviously different from site to site. But at the same time, the overall effect of the random potential is supposed to have been accounted for in the averaged propagator $\hat{G}(z)$. Therefore, we require that the ensemble average of all single-site t-matrices vanishes, i.e.

$$\langle \hat{t}_n \rangle = x \langle \hat{t}_A \rangle + y \langle \hat{t}_B \rangle = 0 \quad (29)$$

Here \hat{t}_A and \hat{t}_B represent the single-site matrix in the case where a given site n is occupied by atom A or B, respectively. $\langle \cdot \rangle$ denotes the averaging over magnon degrees of freedom.

In order to derive the explicit form of the operator \hat{t}_n , we consider the random electron propagator at site n of the interface

$$\hat{G}_n = \frac{1}{\hat{G}^{-1}(z) - \hat{v}_n} = \begin{pmatrix} \hat{G}_n^{++} & \hat{G}_n^{+-} \\ \hat{G}_n^{-+} & \hat{G}_n^{--} \end{pmatrix} \quad (30)$$

The above matrix representation is given with respect to spin up and down subspaces, i.e. $\hat{G}_n^{++} = \langle \hat{t}_n^{++} \rangle$, $\hat{G}_n^{+-} = \langle \hat{t}_n^{+-} \rangle$ and etc. Besides that, we introduce the random "denominator" \hat{D}_n related with the potential \hat{v}_n as

$$\hat{D}_n = \frac{1}{1 - \hat{G}(z) \hat{v}_n} = \begin{pmatrix} \hat{D}_n^{++} & \hat{D}_n^{+-} \\ \hat{D}_n^{-+} & \hat{D}_n^{--} \end{pmatrix} \quad (31)$$

The operators $\hat{G}_n^{(\pm)}$, \hat{G}_n , $\hat{D}_n^{(\pm)}$ and \hat{D}_n are matrices of the dimension (2x2) in the subspace of orbital (s;d). One can also write down the effective random potential $\hat{u}_n = \hat{v}_n$ in the same as (30) and (31) representation in the following form

$$\hat{v}_n = \begin{pmatrix} \hat{J}_n \hat{S} & \hat{J}_n \hat{S}^{\dagger} \\ \hat{J}_n \hat{S}^{\dagger} & \hat{J}_n \hat{S} \end{pmatrix} \quad (32)$$

where

$$\hat{J}_n = \sum_{j; i} f_{j; i} \hat{h}_{j; i} \quad (33)$$

are the operators in the subspace of orbital quantum numbers, given in accordance with (24) and (25). With the use of standard technique for the inversion of matrices in the block form, we have

$$\begin{aligned} \hat{G}_n^{++} &= \frac{1}{\hat{G}^{++}(z) - \hat{J}_n \hat{S} \hat{G}_n^{--} \hat{J}_n} \hat{G}^{++}(z); \\ \hat{G}_n^{+-} &= \frac{1}{\hat{G}^{++}(z) - \hat{J}_n \hat{S} \hat{G}_n^{--} \hat{J}_n} \hat{G}^{+-}(z); \\ \hat{G}_n^{-+} &= \hat{G}_n^{+-} \hat{J}_n \hat{S} \hat{G}_n^{--}; \quad \hat{G}_n^{--} = \hat{G}_n^{--} \hat{J}_n \hat{S} \hat{G}_n^{--}; \end{aligned}$$

where

$$\begin{aligned} \hat{G}_n^{(\pm)} &= \frac{1}{\hat{G}^{(\pm)}(z) - \hat{J}_n \hat{S} \hat{G}_n^{(\pm)} \hat{J}_n} \hat{G}^{(\pm)}(z); \\ \hat{J}_n &= \hat{J}_n \hat{S} \hat{J}_n; \quad \hat{J}_n = \hat{J}_n \hat{S} \hat{J}_n; \end{aligned} \quad (34)$$

Similarly, the elements of \hat{D}_n are written as

$$\begin{aligned}\hat{D}_n^+ &= \frac{1}{\hat{G}_n^+(z)} \hat{\Lambda}_n^+ + \hat{J}_n \hat{n}_+ \hat{G}_n^+ \hat{J}_n^+; \\ \hat{D}_n^\# &= \frac{1}{\hat{G}_n^\#(z)} \hat{\Lambda}_n^\# + \hat{J}_n \hat{n} \hat{G}_n^\# \hat{J}_n^\#; \\ \hat{D}_n^+ &= \hat{G}_n^+ \hat{J}_n^+ \hat{S}_+ \hat{D}_n^\#; \quad \hat{D}_n^\# = \hat{G}_n^\# \hat{J}_n^\# \hat{S}_+ \hat{D}_n^+;\end{aligned}\quad (35)$$

where

$$\hat{G}_n^{(\#)} = \frac{1}{\hat{G}^{(\#)}(z)} \hat{\Lambda}_n^{(\#)} + \hat{J}_n^{(\#)} \hat{n} \hat{G}_n^{(\#)} \hat{J}_n^{(\#)};$$

are the denominators associated with the reduced propagators $g_n^{(\#)}$. Taking into account definition (31), one can write that $\hat{t}_n = \langle \hat{V}_n | \hat{\Lambda}_n^+ \rangle \hat{D}_n^+$. Hence, using (32) and (35), the random single-site transition matrix can be represented in the form

$$\hat{t}_n = \begin{pmatrix} \hat{t}_n^+ & \hat{t}_n^\# \\ \hat{t}_n^\# & \hat{t}_n^+ \end{pmatrix} \quad (36)$$

with respect to spin up and down subspaces, where spin conserving $\hat{t}_n^{(\#)}$ and spin- $\bar{\bar{t}}_n$ parts are given by

$$\begin{aligned}\hat{t}_n^+ &= \hat{\Lambda}_n^+ + \hat{J}_n \hat{n}_+ \hat{G}_n^+ \hat{J}_n^+ \hat{D}_n^+; \\ \hat{t}_n^\# &= \hat{\Lambda}_n^\# + \hat{J}_n \hat{n} \hat{G}_n^\# \hat{J}_n^\# \hat{D}_n^\#; \\ \hat{t}_n^+ &= \hat{G}_n^+ \hat{J}_n^+ \hat{D}_n^\#; \quad \hat{t}_n^\# = \hat{G}_n^\# \hat{J}_n^\# \hat{D}_n^+;\end{aligned}\quad (37)$$

As one can now see, to satisfy the condition (29) one needs to consider only the spin-conserving part of this relation as long as $\hat{t}_n^+ \hat{S}_+ \hat{t}_n^\# = 0$ vanishes since the expression to be averaged contains unequal number of creation and destruction operators of the magnon field. In order to calculate $\hat{t}_n^{(\#)} \hat{t}_n^\#$, one, nevertheless, has to point out the procedure of averaging over magnon degrees of freedom. In our study we adopted the further approximation and assumed, that $\hat{t}_n^+ (\hat{n}_+) \hat{t}_n^\# = \hat{t}_n^+ (n)$ and $\hat{t}_n^\# (\hat{n}) \hat{t}_n^+ = \hat{t}_n^\# (n)$, here $t_n^{(\#)}$ are supposed to be the function of n as they are presented in Exp. (37). $n = n(T)$ is the average number of magnons at the given temperature. In other words we substitute the operators \hat{n} by its average value. The function $n(T)$ is given by the familiar expression

$$n(T) = \frac{Z}{(2\pi)^2} \frac{d^2 q}{e^{\beta \epsilon(q)}} \quad (38)$$

where $\epsilon(q)$ is a surface magnon spectrum. Within this approximation, the system of CPA equations is written in the form

$$\begin{aligned}t_A^+(n)x + t_B^+(n)y &= 0; \\ t_A^\#(n)x + t_B^\#(n)y &= 0;\end{aligned}\quad (39)$$

The quantities $t_n^{(\#)}$ are the (2×2) matrices in the vector space of the orbital quantum numbers ($s; d$). Therefore Exp. (39) represents the system of two (2×2) matrix self-consistency conditions for 8 unknown quantities (z)

in the most general case. They must be solved separately for each interface, as long as Exp. (19) shows that the Green function at the interface depends only on the self-energy correction belonging to the same interface. The system (39) is one of the possible forms of CPA equations but it appears not to be very convenient for the numerical solution and subsequent analysis. For that reasons we employed the augmented space formalism (ASF) by Mookerjee²⁶ and we proceed further along its lines.

Following the ASF, we associate each random variable \hat{V}_n and \hat{J}_n with self-conjugate operators \sim and \bar{J} respectively, which are determined in auxiliary 2-dimensional vector space such a way, that the spectrum of these operators coincides with the set of possible values of these random variables. For the sake of clarity, hereafter, the sign "tilde" is ascribed to any operator acting on the auxiliary space. We also define the orthonormalized basis $|s\rangle$, where $s = A$ or B , which are eigenvectors of \sim and \bar{J} , so that

$$\begin{aligned}\sim |A\rangle &= \epsilon_A |A\rangle; \quad \bar{J} |A\rangle = J_A |A\rangle; \\ \sim |B\rangle &= \epsilon_B |B\rangle; \quad \bar{J} |B\rangle = J_B |B\rangle;\end{aligned}\quad (40)$$

According to that definition \sim and \bar{J} commute with each other. Let now $f(\hat{V}_n; \hat{J}_n)$ be a function or an operator of random variables \hat{V}_n and \hat{J}_n . Then, the operator in the auxiliary space, associated with this function, is defined as $\tilde{f} = f(\sim; \bar{J})$ and according to (40), e.g. $\tilde{f} |A\rangle$ is a value of f , if the site n is occupied by atom A . One can introduce another orthonormal basis in

$$|i\rangle = \frac{1}{\sqrt{x}} |A\rangle + \frac{1}{\sqrt{y}} |B\rangle; \quad |\bar{i}\rangle = \frac{1}{\sqrt{y}} |A\rangle - \frac{1}{\sqrt{x}} |B\rangle;$$

so that the operators \sim and \bar{J} in this representation are written as

$$\sim = \begin{pmatrix} 0 & 1 \\ 1 & 0 \end{pmatrix}; \quad \bar{J} = \begin{pmatrix} J_0 & 0 \\ 0 & J_1 \end{pmatrix}; \quad (41)$$

Here x and y are the concentration of A and B atoms at the interface, respectively, and

$$\begin{aligned}0 &= x \epsilon_A + y \epsilon_B; \quad 1 = y \epsilon_A + x \epsilon_B; \\ &= \frac{1}{xy} (\epsilon_A - \epsilon_B); \quad J_0 = x J_A + y J_B; \\ J_1 &= y J_A + x J_B; \quad \epsilon = \frac{1}{xy} (J_A - J_B);\end{aligned}$$

Then one can prove that the average value of \tilde{f} is given by $f = \langle \tilde{f} \rangle$. Together with the Exp. (41) this property is the way to evaluate the average of any given operator, depending on the random variables, and we proceed further to apply this method to average the matrix (26).

Following the general scheme of ASF, outlined above, the random effective potential $\hat{V}_n = \hat{V}_n^+$ is associated with the operator \tilde{V} acting in the augmented vector space L , where L denotes the 4-dimensional space of orbital ($s; d$) and spin ($\uparrow; \downarrow$) electron degrees of freedom. In accordance with (24), (25) and (41) it has the form

$$\begin{aligned} \hat{U} &\sim \hat{U}_0 + \hat{U}_1 \\ &= \hat{V}_0 + \hat{J}_0 \hat{\sigma} + \hat{V}_1 + \hat{J}_1 \hat{\sigma} \end{aligned} \quad (42)$$

where \hat{V} is defined by (27), operators $\hat{V}_{(i)}$ are defined in the way similar to (24), and other operators are given by

$$\begin{aligned} \hat{V} &= j \hat{S}_+ \hat{S}_- (n) + j \hat{S}_- \hat{S}_+ (n) \\ \hat{J}_i &= J_i \hat{S}_i \quad (i = 0; 1); \end{aligned}$$

We also introduce the nonrandom averaged propagator acting in augmented space

$$\hat{G} = \begin{pmatrix} \hat{G}_0 & 0 \\ 0 & \hat{G}_1 \end{pmatrix}$$

and associated with potential \hat{U} (42) the augmented scattering matrix

$$\hat{\tau} = \hat{U} \sim \frac{1}{1 - \hat{G} \hat{U}} = \begin{pmatrix} \hat{\tau}_{00} & \hat{\tau}_{01} \\ \hat{\tau}_{10} & \hat{\tau}_{11} \end{pmatrix} : \quad (43)$$

Its projection onto the zero-level $\hat{\tau}_{00}$ of the augmented space $\hat{\tau}_{00} = \langle 0 | \hat{\tau} | 0 \rangle$ coincides with the average from the "physical" random matrix (26). Subsequent averaging over magnon degrees of freedom $\langle \hat{\tau}_{00} \rangle_m$ must vanish due to condition (39).

To proceed further, we introduce into consideration the electron propagator \hat{G}_1

$$\hat{G}_1 = \frac{1}{\hat{G}_1 - \hat{U}_1} = \begin{pmatrix} \hat{G}_1^+ & \hat{G}_1^+ \\ \hat{G}_1^+ & \hat{G}_1^+ \end{pmatrix} ;$$

which is connected with the propagation of an electron on the first level of the augmented space in the potential \hat{U}_1 . Taking into account the explicit form of \hat{U}_1 with respect to spin up and down subspaces,

$$\hat{U}_1 = \begin{pmatrix} \hat{V}_1 & \hat{J}_1 \hat{S}_+ \\ \hat{J}_1 \hat{S}_- & \hat{V}_1 \end{pmatrix}$$

where operators \hat{V}_1 and \hat{J}_1 are defined by analogy with (33), one will get

$$\begin{aligned} \hat{G}_1^+ &= \frac{1}{\hat{G}_1^+ - \hat{V}_1} + \hat{J}_1 \hat{S}_+ \hat{G}_1^+ \hat{J}_1^+ \hat{G}_1^+ ; \\ \hat{G}_1^+ &= \frac{1}{\hat{G}_1^+ - \hat{V}_1} + \hat{J}_1 \hat{S}_- \hat{G}_1^+ \hat{J}_1^+ \hat{G}_1^+ ; \\ \hat{G}_1^+ &= \hat{G}_1^+ \hat{J}_1 \hat{S}_+ \hat{G}_1^+ ; \quad \hat{G}_1^+ = \hat{G}_1^+ \hat{J}_1 \hat{S}_- \hat{G}_1^+ ; \end{aligned} \quad (44)$$

where

$$\hat{G}_1^{(\#)} = \frac{1}{\hat{G}_1^{(\#)} - \hat{V}_1^{(\#)}} + \hat{J}_1^{(\#)} \hat{S}_+ \hat{G}_1^{(\#)} \hat{J}_1^{(\#)}$$

and \hat{S}_i are defined in (34). The physical meaning of these formulae is rather transparent. The Green function $\hat{G}_1^{(\#)}$ represents the propagation of the electron in

the spin conserving part of the potential \hat{U}_1 which is $\hat{V}_1^{(\#)}$, while $\hat{G}_1^{(\#)}$ corresponds to scattering on the potential $\hat{V}_1^{(\#)} + \hat{J}_1 \hat{S}_+ \hat{G}_1^{(\#)} \hat{J}_1$, renormalized with respect to the spin-conserving one due to the interaction with magnon subsystem.

After that, we come back to the evaluation of scattering matrix element $\hat{\tau}_{00}$ and introduce the "denominator" \hat{D} , corresponding to the whole augmented potential \hat{U}

$$\hat{D} = \frac{1}{1 - \hat{G} \hat{U}} = \begin{pmatrix} \hat{D}_{00} & \hat{D}_{01} \\ \hat{D}_{10} & \hat{D}_{11} \end{pmatrix}$$

Again, with the use of technique of the inversion of a matrix in the block form and taking into account the elements \hat{U} (42) with respect to auxiliary space, the blocks of \hat{D} can be expressed in terms of propagator \hat{G}_1 as follows

$$\begin{aligned} \hat{D}_{00} &= \frac{1}{1 - \hat{G}_0 \hat{U}_0} + \hat{G}_0 \hat{U}_0 \hat{G}_1^+ \hat{D}_{00} ; \\ \hat{D}_{10} &= \hat{G}_1^+ \hat{D}_{00} ; \quad \hat{D}_{10} = \hat{G}_0 \hat{D}_{11} ; \\ \hat{D}_{11} &= 1 + \hat{G}_0 \hat{G}_1^+ \hat{D}_{00} ; \end{aligned} \quad (45)$$

where we define the propagator \hat{G}_0 , analogous to \hat{G}_1 ,

$$\hat{G}_0 = \frac{1}{\hat{G}_0 - \hat{U}_0} + \hat{G}_0 \hat{U}_0 \hat{G}_1^+ \hat{G}_0 = \begin{pmatrix} \hat{G}_0^+ & \hat{G}_0^+ \\ \hat{G}_0^+ & \hat{G}_0^+ \end{pmatrix} :$$

but corresponding to the propagation of electron in the effective potential \hat{W} , where

$$\hat{W} = \hat{U}_0 + \hat{G}_1^+ \hat{U}_1 = \begin{pmatrix} \hat{W}^+ & \hat{J}_1 \hat{S}_+ \\ \hat{J}_1 \hat{S}_- & \hat{W}^+ \end{pmatrix} : \quad (46)$$

The potential \hat{W} can be seen as renormalization of the "virtual" crystal potential \hat{U}_0 of the zero level of augmented space, representing the average of the random potential of the site. The renormalization comes from the "interaction" \hat{U}_1 in the auxiliary space with the first level, being described by the propagator \hat{G}_1 . Using the explicit form of \hat{U}_1 ,

$$\hat{U}_1 = \begin{pmatrix} \hat{V}_1 & \hat{J}_1 \hat{S}_+ \\ \hat{J}_1 \hat{S}_- & \hat{V}_1 \end{pmatrix} ;$$

one can write down the elements $\hat{W}^{(\#)}$ and \hat{J} as follows

$$\begin{aligned} \hat{W}^{(\#)} &= \hat{V}_0 + \hat{G}_1^{(\#)} \hat{V}_1^{(\#)} + \hat{G}_1^{(\#)} \hat{J}_1 \hat{S}_+ \hat{G}_1^{(\#)} \hat{J}_1^+ \hat{G}_1^{(\#)} \\ &+ \hat{G}_1^{(\#)} \hat{J}_1 \hat{S}_- \hat{G}_1^{(\#)} \hat{J}_1^+ \hat{G}_1^{(\#)} ; \end{aligned}$$

$$\begin{aligned} \hat{J} &= \hat{J}_0 + \hat{G}_1^{(\#)} \hat{J}_1 \hat{S}_+ \hat{G}_1^{(\#)} \hat{J}_1^+ \hat{G}_1^{(\#)} \\ &+ \hat{G}_1^{(\#)} \hat{J}_1 \hat{S}_- \hat{G}_1^{(\#)} \hat{J}_1^+ \hat{G}_1^{(\#)} ; \end{aligned}$$

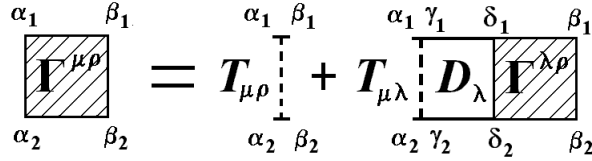


FIG. 3. The diagrammatic representation of the equation (see the text) corresponding to the calculation of vertex part in the "ladder" approximation.

$$\begin{aligned}
 T_{\mu\rho}^{\#} &= x t_A^{\#(n)} t_B^{\#(n)} + y t_B^{\#(n)} t_A^{\#(n)} \\
 T_{\mu\rho}^{\#} &= x n t_A^{+(n)} t_A^{-(n)} + y n t_B^{+(n)} t_B^{-(n)} \\
 T_{\mu\rho}^{\#} &= x n t_A^{-(n)} t_A^{+(n)} + y n t_B^{-(n)} t_B^{+(n)}
 \end{aligned}$$

where $t_{A(B)}^{\#(n)}$ and $t_{A(B)}^{\pm(n)}$ are given by (37). We also define the operator

$$D = \frac{1}{S} G^{-1}(z) G^{-2}(z) \quad (52)$$

denoting the propagator of pair of electrons in the "ladder" equation at z interface. Its definition expresses the fact that in the diagram representation of the CPA approximation the multiple scattering on the given atom is assumed to be incorporated into the single-site t -matrix t_n , corresponding to the single vertex of any diagram. Due to that, the subsequent sites in "ladder" diagrammatic equation (Fig.3) must not reproduce each other. Therefore, the necessary correction is subtracted in Exp. (52). The sum over n is going up to \max similar to Exp. (28). After that definitions the analytical equation for vertex part reads as

$$T_{\mu\rho}^{\#} = T_{\mu\rho}^{\#} + D_{\mu\rho}^{\#} \quad (53)$$

This equation represents the ordinary system of linear equations which easily can be solved. It is also can be proved that a self-energy found in the CPA (50) and the vertex part found in accordance with "ladder" approximation guarantee the Ward's identity (17) mentioned in the previous sections (see details in Appendix A).

III. RESULTS AND DISCUSSION

In this section we present results for the dependence of the TMR amplitude on the parameters $\epsilon_{A(B)}$ of s - d hybridization on interfaces and the temperature variation

of TMR due to excitation of spin- $\uparrow\downarrow$ processes in the system. Assume, that the tunnel junction under consideration is Fe/A₂O₃/Fe three-layer sandwich, and concretize the parameters of Hamiltonian (1). According to estimations of Steams¹⁸, for the itinerant s -like electrons in Fe we chose $k_s^F = 1.09 \text{ \AA}^{-1}$, $k_s^F = 0.42 \text{ \AA}^{-1}$, and $m_s = 1.0 m_e$ (where m_e is bare electron mass). For the more localized d -electrons which should be regarded as holes, we have put $m_d = 10.0 m_e$. Since the density of states at Fermi level for the localized sub-band is larger for the minority spins compared to the majority spins¹⁹, then $k_d^F > k_d^F$, and we chose $k_d^F = 0.5 \text{ \AA}^{-1}$, $k_d^F = 1.4 \text{ \AA}^{-1}$. The values of the Fermi momenta then define the positions of band bottoms V_1, V_3 ($= s, d, = \uparrow, \downarrow$) with respect to Fermi level. We have chosen the values of Fermi momenta such a way that the interfacial densities of states at Fermi level $\rho_{s(d)}^F = 1 = \text{Im } G_{s(d)}(z)$ (where $z = a; b$ are the positions of interfaces) are approximately related as $\rho_s^F : [\rho_s^F - \rho_d^F] : \rho_d^F = 0.1 : 1 : 10$, which is the typical situation for the case of 3d transition metals like Co and Fe [see, for a example, the calculations of Tsymbal and Pettifor¹³].

A₂O₃ tunnel barriers are usually fabricated by glow discharge oxidation of Al layer⁵. The subsequent structural analysis, e.g. by using X-ray photoelectron spectroscopy, shows that alumina, A₂O₃, is amorphous and the obtained A₂O₃ tunnel barrier probably deviates from the ideal A₂O₃ structure⁸. A₂O₃ crystals are found in different structural forms (such as γ , β , and α -A₂O₃)²⁷. With regard to α -A₂O₃, it is known from the band structure calculations²⁸ that the fundamental gap (which is not direct) between the upper valence band and conduction band is of the width of 6.29 eV . The dispersion law in conduction band is not isotropic, and effective electron masses along different directions in Brillouin zone vary from $0.16 m_e$ to $0.40 m_e$ with an average value of about $0.35 m_e$ ²⁸. In the top of the upper valence band, the dispersion curves are very flat, i.e. the effective masses of holes are large compared with the masses of the conduction electrons. Taking into account the previous discussion, we have chosen the following parameters: $U_s = U_d = 3.0 \text{ eV}$ (i.e. the width of the band gap is 6.0 eV , and ϵ_F is assumed to be a zero of energy), $m_s^0 = 0.4 m_e$, $m_d^0 = 10.0 m_e$. Thus, we suppose that both the mostly localized holes as well as itinerant electrons can penetrate into oxide layer. We here note, that as will be seen from the subsequent analysis, the exact value of the large effective mass of holes in A₂O₃ does not influence qualitatively (and even quantitatively) the final results, since the localized holes practically do not contribute into tunneling current, and the similar results can be obtained when one assumes the zero boundary conditions for $G^{\text{ad}}(z; z^0)$ Green function at the interface.

In order to illustrate the general formalism presented in the previous sections, we have considered in particular

the case of only s-d impurity scattering (i.e. $T = 0$ and there are no spin-flip processes) when concentration of both type of atoms at the interface is $x = 50\%$. In this case all formulae have a simple analytical form. Suppose, that $A = B$, then in Eq. (41) we have $G_0 = x A + y B = 0$ and $G^2 = x(1-x)(A-B)^2 = \frac{2}{A}$. Thus, G is the only one parameter describing the amplitude of s-d scattering while the hybridization between bands in the bulk of ferromagnet is supposed to be zero ($V = 0$), because we assume that the effects of hybridization already have been taken into account in calculation of band structure. We also shall omit spin indices as we consider only spin-conserving scattering now. At $x = 50\%$ it turns out that only diagonal elements of the self-energy matrix in sd-space have non-zero value. Then Green functions, e.g. at point a, become

$$\begin{aligned} G^{ss}(a) &= \sum_{k_{max}} \frac{1}{ik_1^s - m_s - \frac{G^s}{m_s^0} G^{ss}(a)} \frac{1}{2} \frac{d}{2}; \\ G^{dd}(a) &= \sum_{k_{max}} \frac{1}{ik_1^d - m_d - \frac{G^d}{m_d^0} G^{dd}(a)} \frac{1}{2} \frac{d}{2}; \end{aligned} \quad (54)$$

and CPA equations are written as follows

$$G^{ss} = \frac{2G^{dd}}{1 + ddG^{dd}}; \quad G^{dd} = \frac{2G^{ss}}{1 + ssG^{ss}} \quad (55)$$

which must be solved self-consistently, e.g. by means of converging iterative procedure. As far as Green functions are diagonal, we introduce $A = G$ and the similar notation for T and D, introduced in section IID. Then

$$T_{sd} = T_{ds} = \frac{2}{j_l + ddG^{dd}} = \frac{2}{j_l + ssG^{ss}}; \quad (56)$$

$$T_{ss} = T_{dd} = 0;$$

$$G^{ss} = \frac{T_{sd}^2 D^{dd}}{1 - T_{sd}^2 D^{ss} D^{dd}}; \quad G^{dd} = \frac{T_{ds}^2 D^{ss}}{1 - T_{ds}^2 D^{ss} D^{dd}};$$

$$G^{sd} = G^{ds} = \frac{T_{sd}}{1 - T_{sd}^2 D^{ss} D^{dd}};$$

Since the mass of holes m_d^0 in oxide is of the order greater than the electron mass m_s^0 , the exponential factor $e^{-2q_2^d(b-a)}$ in formulae (21-23) for tunnel conductance is negligibly small compared with one for s-like electrons. Therefore, one may neglect the contribution of d(holes) into the tunneling current. Then for the conductance of the tunnel junction we obtain

$$G = \sum_{b=a}^X \left(\frac{e^2}{2h} \right)_{0b} A^{ss}(a) \left(\frac{q_2^s}{m_s^0} \right)^2 A^{ss}(b) e^{-2q_2^s(b-a)} \frac{d}{2};$$

where

$$A^{ss}(b) = \frac{e^2}{2h} \sum_{k_{max}} A^{ss}(a) \left(\frac{q_2^s}{m_s^0} \right)^2 A^{ss}(b) e^{-2q_2^s(b-a)} \frac{d}{2} \quad (57)$$

is the conductance corresponding to "bubble" diagram,

$$\begin{aligned} G_a &= \frac{e^2}{2h} \sum_{k_{max}} A^{dd}(a) \frac{d}{2} \left(\frac{q_2^s}{m_s^0} \right)^2 A^{ss}(b) e^{-2q_2^s(b-a)} \frac{d}{2} \\ &+ \frac{e^2}{2h} \sum_{k_{max}} A^{ss}(a) \frac{d}{2} \left(\frac{q_2^s}{m_s^0} \right)^2 A^{ss}(b) e^{-2q_2^s(b-a)} \frac{d}{2} \end{aligned} \quad (58)$$

is the "vertex" contribution to conductance at the left interface, and

$$\begin{aligned} G_b &= \frac{e^2}{2h} \sum_{k_{max}} A^{dd}(b) \frac{d}{2} \left(\frac{q_2^s}{m_s^0} \right)^2 A^{ss}(a) e^{-2q_2^s(b-a)} \frac{d}{2} \\ &+ \frac{e^2}{2h} \sum_{k_{max}} A^{ss}(b) \frac{d}{2} \left(\frac{q_2^s}{m_s^0} \right)^2 A^{ss}(a) e^{-2q_2^s(b-a)} \frac{d}{2} \end{aligned} \quad (59)$$

is the "vertex" contribution to conductance at the right interface. Here A are the transport densities of states which in the present case at the left interface are given by

$$\begin{aligned} A^{ss}(a) &= \frac{k_1^s - m_s}{ik_1^s - m_s - \frac{G^s}{m_s^0} G^{ss}(a)}; \\ A^{dd}(a) &= \frac{k_1^d - m_d}{ik_1^d - m_d - \frac{G^d}{m_d^0} G^{dd}(a)}; \end{aligned} \quad (60)$$

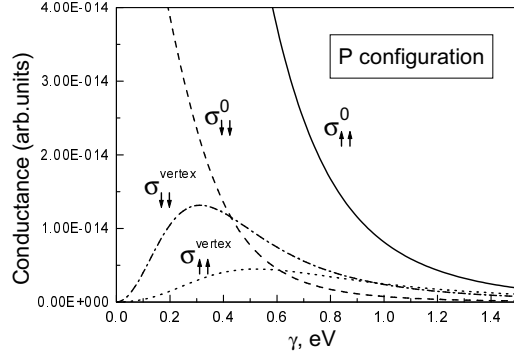


FIG. 4. "Bubble" and vertex contributions to the conductance for the parallel (P) alignment of magnetizations in ferromagnetic layers as a function of the parameter of the random s - d hybridization $\gamma = \gamma_A = \gamma_B$ in the absence of spin- \uparrow processes. The parameters of the model are: s -like electrons $|k_{\uparrow}^F|^s = 1.09 \text{ \AA}^{-1}$, $k_{\uparrow}^F|^s = 0.42 \text{ \AA}^{-1}$, $m_s = 1.0$, $m_s^0 = 0.4$; d -like "holes" $|k_{\downarrow}^F|^d = 0.5 \text{ \AA}^{-1}$, $k_{\downarrow}^F|^d = 1.4 \text{ \AA}^{-1}$, $m_d = m_d^0 = 10.0$, the height of the potential barrier $U_s = U_d = 3.0 \text{ eV}$, the concentration of Fe atoms at the interface $x = 0.5$.

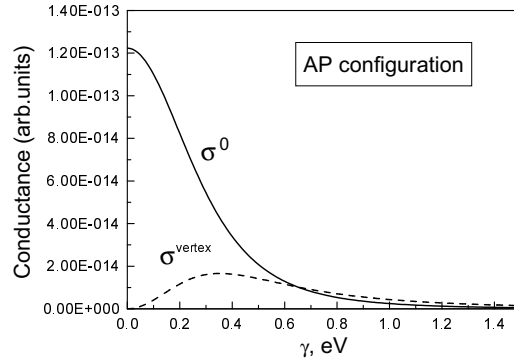


FIG. 5. "Bubble" and vertex contributions to the conductance for the antiparallel (AP) alignment of magnetizations in ferromagnetic layers as a function of the parameter of the random s - d hybridization γ in the absence of spin- \uparrow processes. Parameters of the model are the same ones as in Fig. 4.

and by analogous expressions in case of right interface.

The results of calculations according to these formulae are presented in Figs. 3-7. In Fig. 4 the "bubble" (57) and "vertex" (58, 59) contributions for the up and down spin channels are shown for the parallel (P) alignments of magnetizations in ferromagnetic layers as a function of the parameter of the random s - d hybridization $\gamma = \gamma_A = \gamma_B$ in case of only elastic scattering at the interfaces. The contribution from the "bubble" part is greater for the majority spin (\uparrow) channel since $k_{\uparrow}^F|^s > k_{\downarrow}^F|^s$. On the contrary, the contribution from the vertex correction prevails for the minority spin (\downarrow) electrons. On the first order on γ^2 the imaginary part of the self-energy, which describes the scattering, behaves as

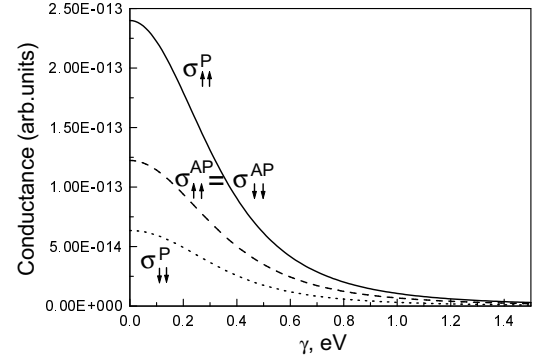


FIG. 6. The conductances of the individual spin channels for the parallel (P) and antiparallel (AP) alignment of magnetizations as a function of the parameter of the random s - d hybridization $\gamma = \gamma_A = \gamma_B$ in the absence of spin- \uparrow processes. The parameters are the same ones as in Fig. 4.

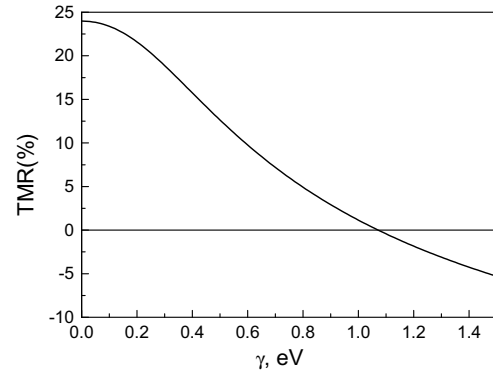


FIG. 7. The tunnel magnetoresistance (TMR) as a function of the parameter of the random s - d hybridization $\gamma = \gamma_A = \gamma_B$ in case of only elastic scattering at the interfaces. The parameters are the same ones as in Fig. 4.

In $\frac{m_s^0}{m_d^0} \approx \frac{1}{10}$ ($\frac{m_s^0}{m_d^0} \approx 10$) [see Exp. (55)]. As far as $\frac{m_s^0}{m_d^0}$ is of the order of magnitude greater than $\frac{m_s^0}{m_d^0}$, s -like itinerant electrons with down spin (\downarrow) scatter in greater extent than electrons with spin up (\uparrow). The transport density of states at the interface $A^{dd}(a)$ (60) is also greater for minority spins. The combination of these factors in final formulae (58), (59) leads to the result that s -like itinerant electrons with minority spin (\downarrow) due to the mechanism of random s - d hybridization give the larger contribution to the diffusive conductance compared with majority spin (\uparrow) electrons.

The "bubble" and vertex contributions to the conductance (which are the same for spin up and spin down channels) for the antiparallel (AP) alignments of magnetizations as a function of γ are presented in Fig. 5. The total conductances for P and AP configurations are shown in Fig. 6. The resulted TMR amplitude as a function of γ is shown in Fig. 7. For the case of absence of s - d hybridization ($\gamma = 0$) we have positive value of TMR $\approx 24\%$ — it is the result of Slonczewski's theory⁹

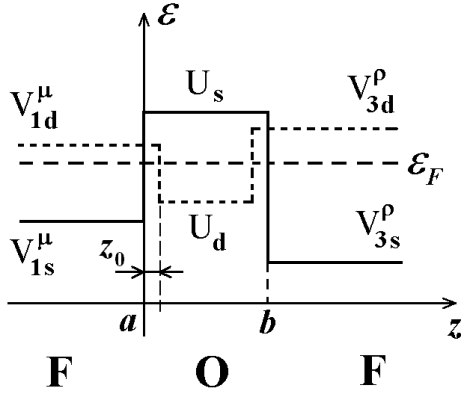


FIG. 8. The corrected model potentials aimed to describe the finite thickness (z_0) of the interface. The notations are similar to ones in Fig. 1.

under the chosen parameters for s-like electrons. With increasing of ϵ_c the TMR amplitude is monotonically decreasing and can become even negative if $\epsilon_c > 0.16$ eV.

Let us now pay attention to the next point. From Fig. 4 it follows that the vertex contributions to conductivity are small compared with the "bubble" contributions due to small value of imaginary part of d-electron Green function (density of states), $\text{Im } G^{dd}(a)$, which determines the "strength" of scattering potential (55). It is the sequence of the restriction of continual type of our model when we neglect the existence of atomic lattice and self-energies have s-like behavior at the interfaces [see Exp. (4)]. In reality, the width of interfacial layer, z_0 , is about the distance between atomic planes or even larger. For the case of bcc lattice, $z_0 = a_0/2$ for [100] direction. One can find, that for the unperturbed d-electron Green function in our model (i.e. when $G^{dd}(a) = 0$), $\text{Im } G_0^{dd}(z = z_0)$ is increasing function in F-layer on the interval of about z_0 from the position of interface $z = a$, and then oscillates near its average value, which is approximately ten times larger than $\text{Im } G_0^{dd}(a)$. The period of oscillations is determined by k_1^d or k_3^d , depending on the electron spin and on the orientation of magnetization in the F-layer. Thus, if one takes into account the non-zero thickness of transition layer, one would expect a more effective mechanism of scattering due to the large value of $\text{Im } G^{dd}$, and the expected value of ϵ_c (at this point TMR = 0) should also be smaller than the above estimated magnitude.

In order to catch the main features of realistic structures and not complicate the model, we have changed only the potential profile for d-holes as it is shown in Fig. 8. As before, $U^d(z)$ has step-like form, but the position of this "step" on both sides of insulating layer is shifted by z_0 from the location of s-like scattering potential. It gives a larger value for $\text{Im } G^{dd}$, and at the same time will not influence substantially on transport properties at small ϵ_c , since d-holes do not give the di-

rect contribution to tunnel current. The potential profile for s-electrons is the same as before in order to obtain the results of Slonczewski's theory for the case of $\epsilon_c = 0$. The changes in formulae for Green functions and conductance are written in Appendix B. The results of calculations are presented in Figs. 9-12. The contribution from vertex correction is now comparable with the "bubble" part of conductance. The TMR amplitude as a function of ϵ_c has the similar behavior as in Fig. 7, and TMR = 0 at $\epsilon_c = 0.16$ eV. Since one can crudely associate the magnitude of the parameter of s-d hybridization with the roughness of the interface structure, then we here point out that the proposed mechanism of random s-d interfacial scattering qualitatively explains the experimental observations that the value of TMR amplitude substantially depends on the conditions of the preparation of the samples^{2,7,8,31}.

To remind in short the experimental situation, we refer to the review by Meservey and Tedrow⁵ where, for example, the results of the early and later measurements of spin polarization P are compared for 3d and rare-earth metals. In early works^{29,30} on tunneling in $\text{Al}/\text{LaO}_3/\text{Ni}$ junctions the analysis of the experimental curves of the dependencies of conductances versus voltage in different magnetic fields gave a value of $P = 11\%$ for Ni. The measurements were also made on Fe, Co, and Gd^{29,30}, and the values obtained for the spin-polarization were, respectively, +44, +34, and +43%. The early experiments were carried out on the junctions which were prepared by oxidizing the Al films in laboratory air saturated with water vapor to form the tunnel barrier and resulted in low values of P for Ni. Later, the improved technique was proposed by Rogers³² when barriers were fabricated in situ with a glow discharge in pure oxygen. Rogers obtained values of polarization for Ni from 17 to 25%. Using this improved technique, Tedrow and Meservey measured spin polarization of Fe, Co, Ni, and Gd, and obtained values (when corrected for spin-orbit scattering) are +40, +35, +23, and +14%, respectively⁵. So, the new technique increased the value of P for Ni and Gd, and also increased the reproducibility of the results. It was conjectured by the authors^{5,32} that in the older method OH ions were presented in the LaO_3 that led to a contamination of the Ni surface. The low values of the early results on the rare-earth metals³³ and their scatter probably also can be explained as the result of surface contamination. For more details, we refer a reader to the original review⁵ and experimental papers^{7,8}.

We have also calculated the temperature dependence of the TMR magnitude taking into account spin- $\uparrow\downarrow$ scattering in addition to s-d impurity scattering as it is described in details in section II C and II D. For that purpose the average magnon number $n(T)$ (38) as a function of the temperature has been found in analogy with Debye's treatment of phonons in the similar way, which was proposed by S. Zhang et al.¹⁶ The magnon dispersion relation in Exp. (38) has been replaced by simple isotropic parabolic spectrum

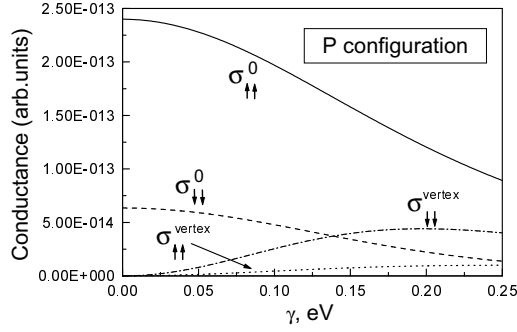


FIG. 9. "Bubble" and vertex contributions to the conductance for the P alignment calculated using the corrected model potential $U_d(z)$ shown in Fig. 8.

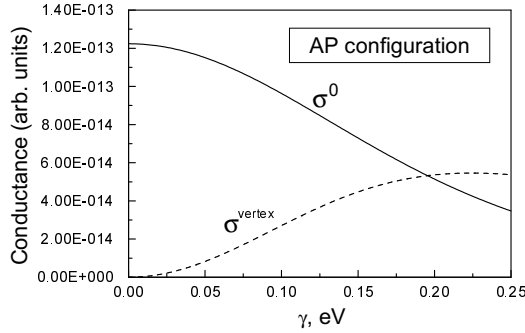


FIG. 10. "Bubble" and vertex contributions to the conductance for the AP alignment calculated using the corrected model potential $U_d(z)$ shown in Fig. 8.

$$k_q = E_m \frac{q}{k_{max}^2};$$

where k_{max} is the equivalent radius of the two-dimensional Brillouin zone (see Exp. 28), and E_m is related to Curie temperature T_c and in the mean-field approximation is given by $E_m = 3k_B T_c / (S + 1)$. For the chosen model of the dispersion relation w_q , one encounters with the divergency on the lower limit of the integral in Exp. 38. Therefore, we have introduced a lower wavelength cutoff E_c ¹⁶. Physically it may represent a finite coherence length due to interfacial roughness. In our calculation we have taken all above mentioned parameters as they were used in paper by S. Zhang et al.¹⁶ for the analysis of the zero-bias anomaly: $S = 3/2$, $k_B T_c = 110$ meV, and $E_c = 4$ meV. Then, for the temperature range within the room value, we have

$$n(T) = \frac{1}{2} \frac{k_B T}{E_m} \log \left(1 + e^{E_c / k_B T} \right);$$

We have put $x = 50\%$, $J_A = 2.0$ eV (for Fe atoms) and $J_B = 0$ eV, i.e. we suppose that spin-flip process is possible, if an electron scatters on the Fe atom. The TMR

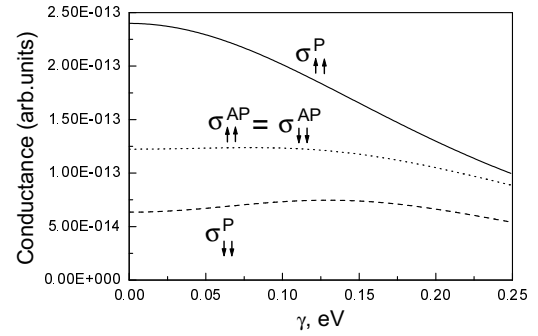


FIG. 11. The conductances of the individual spin channels for the P and AP configurations calculated using the corrected model potential $U_d(z)$ shown in Fig. 8.

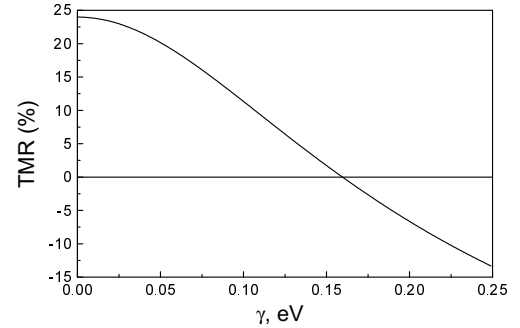


FIG. 12. The TMR as a function of the parameter of the random $s-d$ hybridization calculated with due regard the corrected form of the potential $U_d(z)$.

dependencies on γ at different temperatures $T = 4.2; 77; 210$ and 300 K are plotted on Fig. 13. On Fig. 14 the temperature dependencies of the resistance for the P and AP configurations of magnetization are shown for the same parameters, but $\gamma = 0$. The results show that the TMR amplitude decreases with increasing of the temperature. Moreover, the resistance of the structure for both configurations, P and AP, is also decreasing when temperature increases. It qualitatively agrees with experimental data³⁴. The physical mechanism of this effect is related with excitation of spin-flip processes in the system. Due to these processes, the new channels of electron scattering appear which are frozen at zero temperature. As the result, the conductivity of the system increases for both P and AP configurations. The spin-flip processes mix the channels with "up" and "down" spins. Therefore, the relative difference of the resistances decreases at different configurations and the TMR decreases with increasing of temperature.

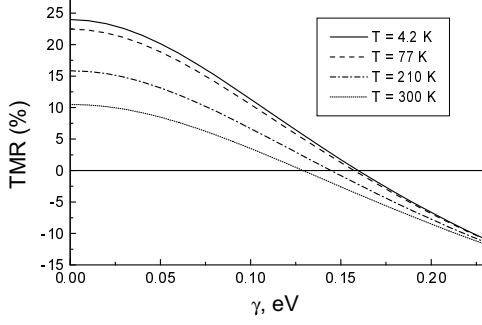


FIG. 13. The TMR as a function of the parameter of the random s d hybridization calculated for different temperatures.

ACKNOWLEDGMENTS

A. Vedyayev and D. Bagrets are grateful to CEA / Grenoble / DRFMC / SP2M / NM for fellowships, A. Bagrets is grateful to Laboratoire Louis Neel (Grenoble, France) for hospitality. This work was partially supported by Russian Foundation for Basic Research (grant No. 98-02-16806).

APPENDIX A: WARD'S IDENTITY

In this Appendix we briefly describe how to obtain Exp. (17) (Ward's identity), and using a simple example we shall show how this identity can be proved.

Starting from Exp. (18), one first has to compute the derivation of the "bubble" conductivity. Assuming, that selfenergy is symmetric with respect to rearrangement of the band indices, i.e. $\Sigma_{\alpha\beta} = \Sigma_{\beta\alpha}$, and using that functions $\psi_i(z^0)$ are the solutions of the Schrödinger equation (5), for the derivation of the current matrix we obtain:

$$\frac{\partial}{\partial z^0} j_{\alpha\beta}(z^0) = \sum_{s;d} 2 \operatorname{Im} \sum_i \psi_i^{\alpha}(z^0) [\psi_i^{\beta}(z^0)]^* ;$$

where

$$\psi_i^{\alpha}(z^0) = \psi_i^{\alpha}(z^0; a) + \psi_i^{\alpha}(z^0; b);$$

and matrix $[\psi_i^{\alpha}(z^0)]$ is defined by Exp. (16). Then, from Exp. (13), (15) we have

$$\begin{aligned} \frac{\partial}{\partial z^0} j_{\alpha\beta}(z; z^0) &= \frac{e^2}{2 \hbar S} \sum_{s;d} \sum_i \psi_i^{\alpha}(z; a) \psi_i^{\beta}(z; b) \\ &+ 2 \operatorname{Im} \sum_i \psi_i^{\alpha}(z^0; b) \psi_i^{\beta}(z; b) : \end{aligned} \quad (\text{A } 1)$$

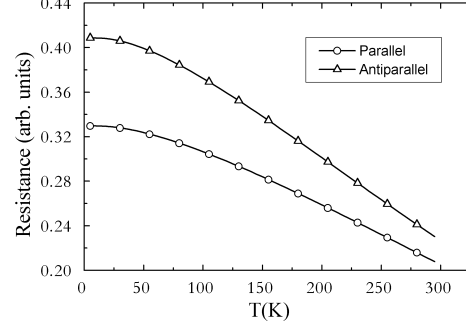


FIG. 14. The temperature dependence of the resistance for P and AP configuration of the magnetizations at $\mu = 0$ and $x = 50\%$.

To proceed further, let us compute the derivation of the vertex correction to conductivity. The initial expression for matrix (see diagram in Fig. 2) is written as

$$j_{\alpha\beta}^{(1)}(a; z^0) = \sum_{s;d} G_{\alpha\beta}^{-1}(a; z^0) \frac{\partial}{\partial z^0} G_{\beta\alpha}^{-1}(z^0; a) :$$

Then, taking into account that Green functions are the solution of the Eq. (3), we obtain

$$\begin{aligned} \frac{\partial}{\partial z^0} j_{\alpha\beta}^{(1)}(a; z^0) &= \sum_{s;d} 2 \operatorname{Im} \sum_i \psi_i^{\alpha}(z^0; a) \psi_i^{\beta}(z^0; a) \\ &+ 2 \operatorname{Im} \sum_i \psi_i^{\alpha}(z^0; a) G_{\alpha\beta}^{-1}(a) G_{\beta\alpha}^{-1}(z^0; a) : \end{aligned}$$

Substituting the obtained expression to formula (14) for the vertex correction, we get

$$\begin{aligned} \frac{\partial}{\partial z^0} j_{\alpha\beta}^{(1)}(z; z^0) &= \frac{e^2}{2 \hbar S^2} \sum_{s;d} \sum_i \psi_i^{\alpha}(z^0; a) \psi_i^{\beta}(z; a) \\ &+ \sum_i \operatorname{Im} G_{\alpha\beta}^{-1}(a) G_{\beta\alpha}^{-1}(z^0; a) : \end{aligned} \quad (\text{A } 2)$$

The sum here is also goes over indices i , j , and k . The similar expression can be written for the derivation of the vertex correction $j_{\alpha\beta}^{(2)}(z; z^0)$ at interface $z = b$. From (A 1) and (A 2) one can simply obtain the final expression (17) for Ward's identity.

Let's prove identity for the simple case of only s d scattering, when there are no spin- \uparrow processes, and $x = 0.5$. This situation was considered in Sec. III, and there were introduced the notations σ , T , and D ($\sigma = s; d$) for the components of the (2×2) matrices σ , T , and D . In these notations, the identity (17), which has to be proved, can be written as

$$\operatorname{Im} \sum_{s;d} \sum_i \psi_i^{\alpha}(z; a) \psi_i^{\beta}(z; b) = \sum_{s;d} \sum_i \operatorname{Im} G_{\alpha\beta}^{-1}(a) \frac{1}{S} G_{\beta\alpha}^{-1}(z^0; a) \operatorname{Im} \sum_{s;d} \sum_i \psi_i^{\gamma}(z; a) \psi_i^{\delta}(z; b) :$$

Here we omitted spin indices, all values are supposed to be taken at interface a or b , G and Γ are defined by Exps. (54, 55). From (52, 53) it follows that

$$D = \frac{1}{S} \sum_j \Gamma_j^2 \Gamma_j^2; \quad \Gamma^1 = T^{-1} D : \quad (56)$$

Using these expressions, Ward's identity can be written in the form:

$$\text{Im } G_{ss}^{(a)} = \sum_{j=1}^N \Gamma_j^2 \Gamma_j^2 + \sum_{j=1}^N \Gamma_j^2 \text{Im } G_{ss}^{(a)} = 0 : \quad (57)$$

Using (56), we then can find

$$\begin{aligned} \text{Im } G_{ss}^{(a)} &= \frac{1}{D_{ss}} \sum_j \Gamma_j^2 \text{Im } G_{ss}^{(a)} + \sum_j \Gamma_j^2 + \sum_j G_{ss}^{(a)} \Gamma_j^2 \text{Im } G_{dd}^{(a)}; \\ \text{Im } G_{dd}^{(a)} &= \frac{1}{D_{dd}} \sum_j \Gamma_j^2 \text{Im } G_{dd}^{(a)} + \sum_j \Gamma_j^2 + \sum_j G_{dd}^{(a)} \Gamma_j^2 \text{Im } G_{ss}^{(a)}; \end{aligned} \quad (58)$$

where

$$D_{ss} = \sum_j \Gamma_j^2 \Gamma_j^2 \Gamma_j^2 + \sum_j \Gamma_j^2 G_{ss}^{(a)} \Gamma_j^2 : \quad (59)$$

The same expressions for $\text{Im } G_{ss}^{(a)}$ and $\text{Im } G_{dd}^{(a)}$ follow directly from the CPA equations (55) — it finishes the proof.

APPENDIX B

Let $x = 0.5$. For potential shown in Fig. 8, the expressions for Green functions at the right interface are given by

$$\begin{aligned} G_{ss}^{(a)} &= \sum_{k=0}^{\infty} \frac{k_1^s}{2m_s} (i \cotan \gamma_1^s)_{ss}^{(a)} \frac{d}{2}; \\ G_{dd}^{(a)} &= \sum_{k=0}^{\infty} \frac{k_1^d}{2m_d} (i \cotan (k_1^d z_0 + \gamma_1^d))_{dd}^{(a)} \frac{d}{2}; \end{aligned} \quad (60)$$

where

$$\tan \gamma_1^s = \frac{k_1^s m_0^s}{q_2^s m_s}; \quad \tan \gamma_1^d = \frac{k_1^d m_0^d}{q_2^d m_d} :$$

and $z_0 = a_0/2$ for bcc lattice of Fe, $a_0 = 2.87 \text{ \AA}$. The similar expressions can be written for the case of left interface. Using these Green functions, for the "transport" densities of states we obtain the following expressions:

$$A_{ss}^{(a)} = \frac{k_1^s m_s}{k_1^s (i \cotan \gamma_1^s) + 2m_s} A_{ss}^{(a)} ; \quad (61)$$

$$A_{dd}^{(a)} = \frac{k_1^d m_d}{k_1^d (i \cotan (k_1^d z_0 + \gamma_1^d)) + 2m_d} A_{dd}^{(a)} ; \quad (62)$$

For the "bubble" part of conductance, instead of Exp. 21, we now have

$$G^0(a; b) = \frac{e^2}{2 h S} \sum_{p=1}^N \frac{q_p}{m_p} A_p^{(a)} A_p^{(b)} ; \quad (63)$$

$$A^T(a) A^{(b)} = \frac{q}{m} A^{(b)} A^{(a)} ; \quad (64)$$

where

$$A_a = \frac{e^{q_2^s z_0}}{0} \frac{0}{d_a} ; \quad A_a = \frac{\sin (k_1^d z_0 + \gamma_1^d)}{\sin \gamma_1^d} ; \quad (65)$$

$$A_b = \frac{e^{q_2^s z_0}}{0} \frac{0}{d_b} ; \quad A_b = \frac{\sin (k_3^d z_0 + \gamma_3^d)}{\sin \gamma_3^d} ; \quad (66)$$

$$\frac{q}{m} = \frac{B}{A} \frac{q_s^0}{m_s^0} e^{q_2^s w} \frac{0}{0} \frac{C}{A} ; \quad (67)$$

and $w = b - a - 2z_0$ is the "width" of d-barrier.

The vertex part of the conductance at point $z = a$ is given by

$$G^a(a; b) = \frac{e^2}{2 h S^2} \sum_{p=1}^N A_p^{(a)} A_p^{(a)} \frac{1}{2} \frac{1}{2} G^0(a; b) ; \quad (68)$$

$$G^a(a; a) = A^{(a)} A^{(a)} ; \quad G^b(b; b) = G^v(a) A^{(a)} \frac{q}{m} A^{(b)} A^{(b)} \frac{q}{m} A^{(a)} G^a(a) ; \quad (69)$$

and the similar expression can be written for the vertex contribution to conductance at the right interface ($z = b$).

- ¹ M. Julliere, Phys. Lett. A, 54, 225 (1975)
- ² J. S. Moodera, L. R. Kinder, T. M. Wong, and R. M. Eservy, Phys. Rev. Lett., 74, 3273 (1995); J. S. Moodera, L. R. Kinder, J. Appl. Phys., 79, 4724 (1996); J. S. Moodera, J. Nowak, and R. J. M. van de Veerdok, Phys. Rev. Lett., 80, 2941 (1998)
- ³ T. Miyazaki, N. Tezuka, J. Magn. Magn. Mater., 139, L231 (1995); N. Tezuka and T. Miyazaki, J. Appl. Phys., 79, 6262 (1996); T. Miyazaki, S. Kumagai, T. Yaei, J. Appl. Phys., 81, 3753 (1997)
- ⁴ W. J. Gallagher, S. S. P. Parkin, Yu Lu, X. P. Bian, A. Marley, K. P. Roche, R. A. Altman, S. A. Rishton, C. Jahnes, T. W. Shaw, and G. Xiao, J. Appl. Phys., 81, 3741 (1997)
- ⁵ R. Meservy and P. M. Tedrow, Phys. Rep., 238, 173 (1994)
- ⁶ S. Zhang and P. M. Levy, Eur. Phys. J. B, 10, 599 (1999)
- ⁷ J. S. Moodera, E. F. Gallagher, K. Robinson, and J. Nowak, Appl. Phys. Lett., 70, 3050 (1997)
- ⁸ T. Mitsuzuka, K. Matsuda, A. Kamijō, and H. Tsuge, J. Appl. Phys., 85 5807 (1999)
- ⁹ C. Slonczewski, Phys. Rev. B, 39 6995 (1989);
- ¹⁰ A. M. Bratkovsky, Pis'ma Zh. Eksp. Teor. Fiz., 65 (5) 430 (1997) [JETP Letters, 65 (5), 452 (1997)]
- ¹¹ W. H. Butler, X. G. Zhang, X. Wang, J. V. Ek, and J. M. MacLaren, J. Appl. Phys., 81, 5518 (1997); J. M. MacLaren, W. H. Butler, and X. G. Zhang, J. Appl. Phys., 81, 6521 (1998)
- ¹² J. Mathon, Phys. Rev. B, 56, 11810 (1997)
- ¹³ E. Yu. Tsymbal and D. G. Pettifor, J. Phys.: Condens. Matter., 9, L4 (1997)
- ¹⁴ J. M. De Teresa, A. Barthelmy, A. Fert, J. P. Contour, R. Lyonnet, F. Montaigne, P. Seneor, and A. Vaures, Phys. Rev. Lett., 82, 4288 (1999)
- ¹⁵ E. Yu. Tsymbal and D. G. Pettifor, Phys. Rev. B, 58, 432 (1998)
- ¹⁶ S. Zhang, P. M. Levy, A. C. Marley, and S. S. P. Parkin, Phys. Rev. Lett., 79, 3744 (1997)
- ¹⁷ A. Vedyayev, N. Ryzhanova, R. V. Lutters, and B. Dieny, Europhys. Lett., 46, 808 (1998)
- ¹⁸ M. B. Steams, J. Magn. Magn. Mater., 5, 167 (1977)
- ¹⁹ D. A. Papaconstantopoulos, Handbook of the Band Structure of Elemental Solids (Plenum, New York, 1986)
- ²⁰ F. Bruekers, A. Vedyayev, M. Giorgino, Phys. Rev. B, 7, 380 (1973)
- ²¹ R. Kubo, M. Toda and N. Hashitsume. Statistical Physics II. Nonequilibrium Statistical Mechanics. (Springer, Berlin, 1985)
- ²² A. Vedyayev, N. Ryzhanova, C. Lacroix, L. Giacomoni, and B. Dieny, Europhys. Lett., 39, 219 (1997)
- ²³ P. Soven, Phys. Rev. B, 156, 809 (1967)
- ²⁴ P. M. Levy, H. E. Camblong, and S. Zhang, J. Appl. Phys., 75, 7076 (1994); P. M. Levy, Solid State Phys., 47, 367 (1994)
- ²⁵ B. Velicky, Phys. Rev. B, 184, 614 (1969)
- ²⁶ A. Mookerjee, J. Phys. C, 6, L205, 1340 (1973)
- ²⁷ S. Ciraci, I. P. Barta, Phys. Rev. B, 28, 982 (1983)
- ²⁸ Y. N. Xu, W. Y. Ching, Phys. Rev. B, 43, 4461 (1991)
- ²⁹ P. M. Tedrow and R. Meservy, Phys. Rev. B, 7, 318 (1973)
- ³⁰ R. Meservy and P. M. Tedrow, Solid State Commun., 11, 333 (1972)
- ³¹ M. Covington, J. Nowak, and D. Song, Appl. Phys. Lett., 76, 3965 (2000); R. C. Sousa, J. J. Sun, V. Soares, P. P. Freitas, A. Kling, M. F. da Silva, and J. C. Soares, Appl. Phys. Lett., 73, 3288 (1998); J. J. Sun, V. Soares, and P. P. Freitas, Appl. Phys. Lett., 74, 448 (1999)
- ³² J. S. Rogers, private communication, 1978
- ³³ R. Meservy, D. Paraskevopoulos, and P. M. Tedrow, Phys. Rev. B, 22, 1331 (1980)
- ³⁴ Yu Lu, X. W. Li, Gang Xiao, R. A. Altman, W. J. Gallagher, A. Marley, K. Roche, S. Parkin, J. Appl. Phys., 83, 6515 (1998)